

Microscopic three-body force for asymmetric nuclear matter

W. Zuo

Institute of Modern Physics, Chinese Academy of Sciences, 730000 Lanzhou, China

A. Lejeune

Institut de Physique, B5 Sart-Tilman, B-4000 Liège 1, Belgium

U. Lombardo¹

Dipartimento di Fisica, 57 Corso Italia, and INFN-LNS, 44 Via Santa Sofia 95125 Catania, Italy

J. F. Mathiot

Laboratoire de Physique Corpusculaire, Université Blaise-Pascal, CNRS-IN2P3, 24 Avenue des Landais, F-63177 Aubiere Cedex, France

(Preliminary draft: November 14, 2018)

Abstract

Brueckner calculations including a microscopic three-body force have been extended to isospin asymmetric nuclear matter. The effects of the three-body force on the equation of state and on the single-particle properties of nuclear matter are discussed with a view to possible applications in nuclear physics and astrophysics. It is shown that, even in the presence of the three-body force, the empirical parabolic law of the energy per nucleon vs isospin asymmetry $\beta = (N - Z)/A$ is fulfilled in the whole asymmetry range $0 \leq \beta \leq 1$ up to high densities. The three-body force provides a strong enhancement of symmetry energy increasing with the density in good agreement with relativistic approaches. The Lane's assumption that proton and neutron mean fields linearly vary vs the isospin parameter is violated at high density in the presence of the three-body force. Instead the momentum dependence of the mean fields is rather insensitive to three body force which brings about a linear isospin deviation of the neutron and proton effective masses. The isospin effects on multifragmentation events and collective flows in heavy-ion collisions are briefly discussed along with the conditions for direct URCA processes to occur in the neutron-star cooling.

PACS numbers: 25.70-z, 13.75.Cs, 21.65.+f, 24.10.Cn

Keywords: three body force, asymmetric nuclear matter, isospin

¹ e-mail: lombardo@lns.infn.it

1. Introduction

The equation of state (EOS) of neutron-rich matter is a source of important theoretical predictions on the properties of neutron stars, heavy-ion collisions (HIC) and nuclei at the neutron drip line [1]. The interest has been mainly focussed on the properties of the symmetry energy, including its dependence upon the baryonic density. Studies of neutron-star cooling [2], spin-polarized states [3], collective flows and isospin distillation in HIC [4–6] have stressed that those phenomena are very sensitive to the values of the symmetry energy in the respective density domains. The EOS of isospin-asymmetric nuclear matter has been recently studied in the framework of the Brueckner-Bethe-Goldstone (BBG) theory [7,8]. The convergence of the BBG hole-line expansion has been assessed in recent times with high accuracy [9], even if the the saturation properties of nuclear matter are not reproduced. It is commonly recognized that the missing saturation is due to the model of nucleons as structureless particles interacting via a bare two-body force (2BF) and one has to introduce three-body forces (3BF). The first microscopic model of 3BF was the Fujita-Miyazawa model [10] where the isobar $\Delta(1232)$ is excited in a pion exchange interaction between two nucleons. The model was later extended to the $N(1440)$ Roper resonance [11]. It has been also recognized that the main relativistic effect introduced by Dirac-Brueckner approach is the excitation of the negative energy states of the Fermi sea which can be described in terms of a 3TB [12] as well.

The above mentioned 3BF components have a strong saturating effect as already shown by a Brueckner-Hartree-Fock (BHF) calculation with the Paris potential as 2BF [11]. This 3BF has been re-adopted in Ref. [13] in combination with the Argonne V_{18} [14] as two-body component. In Ref. [15] it was discussed the EOS of pure neutron matter and a preliminary prediction for the symmetry energy based on the shift between the energy of pure neutron matter and symmetric nuclear matter. But one may argue that 3BF could modify the β^2 law fulfilled by the binding energy of asymmetric nuclear matter specially at high density and higher order terms in the β expansion could significantly limit the role played by the symmetry energy in describing the isospin effects. All that required to extend the calculation of the EOS to the full range $0 < \beta < 1$ in a baryonic density range high enough. In this paper we present the results of such a calculation. After describing the model of TBFB (Sec. 2) we will focus on the 3BF effects on binding energy, symmetry energy and single-particle properties of asymmetric nuclear matter (Sec. 3). Then a few direct applications in the neutron star cooling and in the isospin properties of HIC will be shortly discussed along with a comparison with other approaches (Sec. 4).

2. Isospin dependent 3BF

The microscopic 3BF adopted in the present calculation is based on the meson-exchange current approach. It is described in full detail in Ref. [11]. The new meson parameters calculated to meet the self-consistent requirement with the adopted AV_{18} 2BF are reported in Ref. [13].

It has been shown [11,13] that the main contributions to 3BF rise from the two-meson exchange part of the NN interaction medium modified by the intermediate virtual excitation of nucleon resonances (isobar $\Delta(1232)$ and Roper $N(1440)$) (Fig. 1a) and from the two-meson exchange part with nucleon-antinucleon virtual excitation (Fig. 1d). This latter contains the relativistic effects associated to the dressed spinors of the Dirac-Brueckner approach [16]. The terms associated to the non-linear π -nucleon coupling required by the chiral symmetry

[17] play a minor role specially above the saturation density, where heavy mesons (σ and ω) are dominating over the 2π -3BF (Fig. 1b, diagrams without heavy mesons). The contribution due to meson-meson coupling (Fig. 1c) is also negligible [11] and was not considered in the present calculation. In the context of non relativistic approaches phenomenological 3BF have also been introduced [18] in the calculations of nuclear matter. They are modelled on the saturation properties of nuclear matter and/or binding energies of light nuclei. A good agreement between microscopic and phenomenological 3BF is found only when this latter is treated within the Brueckner approach [19].

The general Brueckner formalism for asymmetric nuclear matter (ANM) with 2BF's is described in Ref. [8]. The rigorous procedure to include 3BF would require to solve the Bethe-Faddeev equation with a 3BF much the same as already done to calculate the three-body clusters in the BBG hole-line expansion [9]. But at this moment this appears a formidable task and we are content to follow a simplified procedure based on converting the 3BF into an effective two-body force via a suitable integration over the third-nucleon degrees of freedom. The integral is weighted over the correlation function of the third nucleon with the two others [11,13]. The effective 2BF for asymmetric nuclear matter is defined as

$$\begin{aligned} \langle \vec{r}_1 \vec{r}_2 | V_3^{\tau_1 \tau_2} | \vec{r}'_1 \vec{r}'_2 \rangle &= \frac{1}{4} \sum_{\tau_3} \sum_{\sigma_3} \sum_n \int d\vec{r}_3 d\vec{r}'_3 \phi_n^*(\tau_3 \vec{r}'_3) (1 - \eta_{\tau_1, \tau_3}(r'_{13})) (1 - \eta_{\tau_2, \tau_3}(r'_{23})) \\ &\times W_3(\vec{r}'_1 \vec{r}'_2 \vec{r}'_3 | \vec{r}_1 \vec{r}_2 \vec{r}_3) \phi_n(\tau_3 r_3) (1 - \eta_{\tau_1, \tau_3}(r_{13})) (1 - \eta_{\tau_2, \tau_3}(r_{23})) \end{aligned} \quad (1)$$

The function $\eta_{\tau_1 \tau_2}(r)$ is the average over spin and momenta in the Fermi sea of the defect function, of which only the most important partial wave components have been included, i.e. the 1S_0 and 3S_1 partial waves.

The transformation of the 3BF to an effective 2BF entails a selfconsistent coupling between 3BF and Brueckner procedure of solving the Brueckner-Bethe-Goldstone equations. One first calculates the correlation function with only the 2BF and then builds up the effective 3BF which in turn is added to the 2BF, and again calculates the correlation function and so on up to the convergence is reached. As previously mentioned the bare 2BF adopted in the calculations was the charge dependent AV_{18} . The partial wave expansion of full interaction has been truncated at $l_{max} = 6$.

3. Numerical results

The EOS of ANM has been calculated spanning the whole asymmetry range with a step-size $\Delta\beta = .2$ and a density domain up to 0.45fm^{-3} . The case of symmetric nuclear matter ($\beta = 0$) is discussed in Ref. [15] (the saturation properties are reported in Table 1). The results for ANM are displayed in Fig. 2 for both cases with (left panel) and without (right panel) the 3BF. In the figure energy shift for asymmetric-to-symmetric nuclear matter is reported versus β^2 . The individual runs (symbols in the Figure) are depicted along with their linear fits (solid lines) performed with only the first three values of asymmetry parameter β . From the comparison between the two sets of calculations one may notice that, despite its strongly density dependent repulsive effect, the 3BF does not violate the β^2 law fulfilled already with only 2BF. The rather good agreement between the symbols and the corresponding lines (maximum deviation is 6%) indicates the high quality of the β^2 law up to the largest densities. This is a quite astonishing result because the 3BF introduces a strong density and isospin dependence, making the nucleon-nucleon (NN) interaction quite different from the pure 2BF. On the other hand, it is a quite desirable result indeed for

two reasons. First, this (in agreement with previous studies [7,8,20,21] using alone charge-independent 2BF) provides a strong support to the applications based on the EOS of *AMN* extracted from the empirical β^2 -law. Second, it imposes also strict theoretical constraints on the phenomenological nuclear forces when extended to *AMN*. We have in mind the Skyrme forces which have been fit around the saturation point of symmetric nuclear matter and include an effective density-dependent term to simulate the effects of 3BF.

In Table 1 the saturation properties of ANM are shown with and without 3BF. One may just notice that the compression modulus results smaller with 3BF despite the strong enhancement of the curvature of the EOS. This is due to the fact that it is also proportional to the square of the saturation density, which turns out to be very much reduced.

The symmetry energy is defined as

$$E_{sym}(\rho) = \frac{1}{2} \left[\frac{\partial^2 B(\rho, \beta)}{\partial \beta^2} \right]_{\beta=0}. \quad (2)$$

Due to the simple β^2 -law the symmetry energy can be equivalently calculated as the difference between the energy per nucleon of pure neutron matter and symmetric nuclear matter, i.e.,

$$E_{sym}(\rho) = E_A(\rho, 1) - E_A(\rho, 0). \quad (3)$$

Fig. 3 shows the effect of the 3BF on the symmetry energy in the density domain considered in this study. At the saturation density the two values do not significantly differ: 30.71 MeV (3BF included) and 29.28 MeV (no 3BF). Both are in good agreement with the empirical value $30. \pm 4$ MeV extracted from the nuclear mass table [22]. Above ρ_0 the 3BF gives a strong enhancement of symmetry energy since it is strongly repulsive at high density. Both curves, with and without the 3BF, have been parametrized by simple power laws as follows,

- BHF with pure AV_{18} 2BF

$$E_{sym} = 30.7u^{0.58} \quad (4)$$

- BHF using AV_{18} plus the 3BF

$$\begin{aligned} E_{sym} &= 30.71u^{0.6} & u \leq 1 \\ &= 30.71 + 18.42(u - 1) + 9(u - 1)^2 & u > 1 \end{aligned} \quad (5)$$

where $u = \rho/\rho_0$, and $\rho_0 = 0.17 \text{ fm}^{-3}$ the empirical saturation density. The above simple relations, plotted in Fig. 3 (right panel), may be useful in HIC simulations.

In Fig. 3 (left panel) E_{sym} vs density is compared with other approaches. Despite the overall agreement with the predictions of both relativistic mean-field (RMF) theory [23] and Dirac-Brueckner-Hartree-Fock approach (DBHF) [20], the density dependence is found to be rather different. Both RMF and DBHF theories predict an almost linear variation of E_{sym} vs. density. Instead, the present BHF calculation with the 3BF gives a slower varying

E_{sym} vs. ρ at relatively low densities, say from $\rho \simeq 0.03\text{fm}^{-3}$ to $\rho \simeq 0.25\text{fm}^{-3}$. Such a slow variation vs. density is also found in a density region up to $\rho \simeq 0.2\text{fm}^{-3}$ in Ref. [24] from the three-loop approximation of chiral perturbation theory. In this density region, the shape of E_{sym} plays an important role as to the study of the isospin effects in HIC at intermediate energy as discussed later. On the contrary, in the relatively high density domain, i.e., $\rho \geq 0.3\text{fm}^{-3}$, the present calculation predicts a steeper density dependence of E_{sym} than DBHF and RMF.

Due to the isospin effect the proton and neutron single-particle potentials are different. As discussed in Ref. [8] where only the charge-independent AV_{14} 2BF was used, the attractive $T = 0$ SD channel contribution in the two-body NN interaction mainly drives the isospin dependence of the proton and neutron mean fields. As a result, the proton mean field becomes more attractive while the neutron one more repulsive as increasing asymmetry. In the BHF approximation both mean fields vary linearly with the asymmetry parameter β , which is in keeping with the β^2 dependence of the energy per particle. A potential linearly dependent on β was introduced phenomenologically long ago [25] and is referred to as Lane potential. Due to the importance of the single-particle properties such as mean field and effective mass in HIC physics [26,27], it is of some interest to explore the effect of the 3BF on such quantities. The proton and neutron mean fields are shown as a function of momentum k at different asymmetries $\beta = 0, 0.2, 0.4, 0.6, 0.8$ in Fig. 4 for the saturation density $\rho = 0.17\text{fm}^{-3}$ and in Fig. 5 for high density $\rho = 0.34\text{fm}^{-3}$. In both figures the left panels display the results using AV_{18} plus the 3BF and the right panels those using pure AV_{18} . As expected, the 3BF adds a repulsive contribution to both proton and neutron mean fields at all asymmetries. At relatively low density (Fig. 4), the proton mean field with 3BF becomes more attractive, which is in agreement with the 2BF prediction. However the validity of the linear Lane assumption is broken by 3BF as more clearly seen in the left panel of Fig. 6, where the isospin variation of the proton and neutron mean fields are plotted at momentum $k = 0$. At relatively high density (Figs. 5 and 6), the 3BF force effect becomes much more pronounced and in fact it brings a strong deviation from the linear Lane assumption. The neutron mean field rises up more rapidly as compared to the results with pure AV_{18} . The same happens to the proton potential which at a certain asymmetry becomes even more repulsive. This remarkable result can be explained by the competition between the isospin dependence of the 3BF and the contribution from the attractive $T = 0$ SD channel. As increasing isospin asymmetry the 3BF repulsion starts to compete with the $T = 0$ SD channel 2BF attraction, and becomes the dominant one at density high enough.

The effective mass, which is related to the non-locality (momentum dependence) of the neutron and proton mean fields, is defined as

$$\frac{m_{\tau}^{*}(k)}{m} = \frac{k}{m} \left(\frac{dE^{\tau}(k)}{dk} \right)^{-1}. \quad (6)$$

The momentum dependence of m^{*} is featured by a wide bump inside the Fermi sphere due to the high probability amplitude for particle-hole excitations near the Fermi surface [28]. The isospin dependence of the proton and neutron effective masses at their respective Fermi momentum k_F^p and k_F^n are given in the right panel of Fig. (6). The 3BF does not affect the linear scissor-shaped behavior observed in the previous calculations using a pure 2BF [7,8]. One should notice that the isospin effect on neutron and proton effective masses

in the Brueckner approach goes the other way around than in the RMF approach [23]. This discrepancy is to be understood taking also into account the different definitions of effective mass in the two approaches.

4. Summary and discussion

In the present work the microscopic 3BF based on meson-exchange current approach has been extended and applied to isospin ANM in the framework of the Brueckner theory. The 3BF effects on the isospin dependence of both the nuclear EOS and single-particle properties have been investigated.

The results confirm the validity of the β^2 law for the energy per nucleon in the entire range of isospin asymmetry and up to high density in spite of the strong isospin and density dependence of the 3BF. As a consequence the isospin effects in ANM are just driven by the symmetry energy as in the case with only the 2BF. The vanishing of higher powers in the β^2 expansion also supports the simple recipe often adopted to extract the symmetry energy from the two limiting cases of symmetric nuclear matter and pure neutron matter. It also constraints theoretically the phenomenological interactions, such as the Skyrme forces which take into account the effect of 3BF by a density dependent term.

As expected, the 3BF improves the saturation properties of symmetric nuclear matter by shifting the equilibrium density close to the empirical value. At relatively low density, the 3BF effect on the nuclear symmetry energy is quite small. On the contrary, at high density, it brings a strong enhancement and consequently the symmetry energy rises with density more steeply than the corresponding 2BF prediction. The non linear increase of symmetry energy at high density has also been observed in a recent relativistic Hartree-Fock calculation [23] as the ‘Fock’ exchange effect of the non linear scalar self-interactions. But in the same Ref. [23], it is also shown that at sub-nuclear densities, the Fock contribution could result in a softening of the symmetry potential term.

The density dependence of the symmetry energy has been parametrized for the sake of application in HIC with very neutron-rich ions. It has been shown already that isospin fractionation [4,29] in multifragmentation events is very sensitive to the density dependence of E_{sym} in the low density region. In particular, in Ref. [30] is shown that using an isospin stiff nuclear EOS with symmetry energy curvature equal to -69 MeV (very close to the present value of -66 MeV) leads to a remarkable value for the liquid-to-gas isospin asymmetry ratio which is consistent with the experimental prediction [5]. An isospin scaling has been proposed in multifragmentation events of HIC, which turns out to be also very sensitive to the density dependence of E_{sym} . Using the expanding evaporating source model and adopting for E_{sym} the simple parametrization $C \cdot (\rho/\rho_0)^\gamma$ the fragment data can be fairly well reproduced by taking $\gamma = 0.6$ [31], which coincides with the fit of our microscopic value (cfr. Eq. (5)).

The preequilibrium particle emission [32,33] and collective flows [4,6] can instead probe the symmetry energy in the range of high density, say up to two times the saturation density, but only with an isospin stiff EOS which is in agreement with our prediction.

In the high density range the symmetry energy is also relevant to the study of the neutron-star properties such as the cooling mechanism. In fact, a steep increase of E_{sym} with density favours the direct URCA processes [2]. In Fig. 7 the proton fraction is reported for β -equilibrium nuclear matter in different approximations. The threshold of direct URCA processes is only crossed by the results with 3BF at a reasonable value of the neutron-star

density.

As to the single-particle properties, the effect of the 3BF is to add an extra repulsion to both proton and neutron mean fields so that the linear Lane assumption breaks down slightly around the saturation density but quite strongly at high density. However, the scissor-shaped behavior of the proton and neutron effective masses vs. β remains unchanged being the momentum dependence of the mean fields rather insensitive to 3BF. In a calculation not reported here it was found that the 3BF affects only slightly the *rearrangement* contribution to the nuclear mean field and can not improve the fulfillment of Hughenoltz-Van Hove theorem (see Ref. [8]). This requires to go beyond BHF approximation in the expansion of mass operator that is a work still in progress.

Acknowledgments:

One of us (W. Z.) would like to thank INFN-LNS and the Physics Department of the Catania University (Italy) for their hospitality during the preparation of the present work.

This work has been supported in part by the Chinese Academy of Science, within the *one Hundred Person Project*, the Major State Basic Research Development Program of China under No. G2000077400.

REFERENCES

- [1] For a recent review see: *Nuclear Methods and the Nuclear Equation of State*, M. Baldo Editor (World Scientific, 1999).
- [2] J. M. Lattimer, C.J. Pethick, M. Prakash and P. Haensel, Phys. Rev. Lett. **66**, 2701 (1991).
- [3] J. Margueron, PhD Thesis, IPNO-T-01-07 (2001).
- [4] B.A. Li, Phys. Rev. Lett. **85**, 4221 (2000).
- [5] H.S. Xu et al., Phys. Rev. Lett. **85**, 1908 (2000).
- [6] L. Scalone, M. Colonna and M. Di Toro, Phys. Lett. **B 461**, 9 (1999).
- [7] I. Bombaci and U. Lombardo, Phys. Rev. **C 44**, 1892 (1991).
- [8] W. Zuo, I. Bombaci and U. Lombardo, Phys. Rev. **C 60**, 024605 (1999).
- [9] H.Q.Song, M.Baldo, G.Giansiracusa and U.Lombardo, Phys. Rev. Lett. **81**, 1584 (1998); M.Baldo, G.Giansiracusa, U.Lombardo and H.Q. Song, Phys. Letters **B 473**, 1 (2000).
- [10] J. Fujita and H. Miyazawa, Prog. Theor. Phys. **17**, 360 (1957); **17**, 366 (1957).
- [11] P. Grange, A. Lejeune, M. Martzloff, and J. -F. Mathiot, Phys. Rev. **C40**, 1040 (1989).
- [12] G.E. Brown, W. Weise, G. Baym and J. Speth, Comments Nucl. Phys. **17**, 39 (1987).
- [13] W. Zuo, A. Lejeune, U. Lombardo, J.-F. Mathiot, PP 2002, (submitted to Nuclear Physics).
- [14] R.B. Wiringa, V.G.J. Stoks, R. Schiavilla, Phys. Rev.**C 51**, 38 (1995) .
- [15] A. Lejeune, U. Lombardo and W. Zuo, Phys. Lett. **477**, 45 (2000).
- [16] R. Brockmann and R. Machleidt, 'The Dirac-Brueckner Approach' in *Nuclear Methods and Nuclear Equation of State*, Ed. M. Baldo (World Scientific,1999) p.121.
- [17] E. Epelbaum, Ulf-G. Meissner, W. Glöckle, C. Elster, H. Kamada, A. Nogga, H. Witala, Proc. Conference on "Mesons and Light Nuclei", Prag, July 2001, and references therein quoted, nucl-th/0109065.
- [18] For a recent review see: S.C. Pieper, V.R. Pandharipande, R.B. Wiringa, and J. Carson, Phys. Rev. C **64**, 014001 (2001).
- [19] M. Baldo, I. Bombaci and G.F. Burgio, Astron. Astrophys. **328**, 274 (1997).
- [20] C.H. Lee, T.T.S. Kuo, G. Q. Li and G.E. Brown, Phys. Rev. **C 57**, 3488 (1998).
- [21] H. Huber, F. Weber and M.K. Wiegel, Phys. Rev. **C 51**, 1790 (1995); Phys. Rev. **C 57**, 3484 (1998).
- [22] P. E. Haustein, At. Data Nucl. Data Tables **39**, 185 (1988).
- [23] B. Liu, V. Greco, F. Matera, M. Colonna, M. Di Toro (to be published in Phys. Rev. **C 65** March 2002).
- [24] N. Kaiser, S. Fritsch and W. Weise, 'Chiral Dynamics and Nuclear Matter', arXiv:nucl-th/0105057.
- [25] A.M. Lane, Nucl. Phys. **35**, 676 (1962).
- [26] G. F. Bertsch and S. Das Gupta, Phys. Rep. **160**, 189 (1988).
- [27] W. Cassing, V. Metag, U. Mosel and K. Nitta, Phys. Rep. **188**, 363 (1990).
- [28] J. P. Jeukenne, A. Lejeune and C. Mahaux, Phys. Rep. **25 C**, 83 (1976).
- [29] M. Colonna, M. Di Toro, A.B. Larionov, Phys. Lett. **B428**, 1 (1998).
- [30] B. A. Li and C. M. Ko, Nucl. Phys. **A 618**, 498 (1997).
- [31] M.B. Tsang, W.A. Friedman, C.K. Gelbke, W. G. Lynch, G. Verde and H. Xu, Phys. Rev. Lett.**86**, 5023 (2001).
- [32] B.A. Li, C.M. Ko and W. Bauer, Inter. J. Mod. Phys. **E 7**, 147 (1998).

- [33] B.A. Li, C.M. Ko and Z.Z. Ren, Phys. Rev. Lett. **78**, 1644 (1997).
[34] R.B. Wiringa, V. Fiks and A. Fabrocini, Phys. Rev. **C 38**, 1010 (1988).

Tab. 1 - Equilibrium density of asymmetric nuclear matter, incompressibility and energy per nucleon at equilibrium density corresponding to four different values of asymmetry β .

β	$AV_{18} + 3BF$			AV_{18}		
	ρ_{eq}	$K(\rho_{eq})$	$E_A(\rho_{eq})$	ρ_{eq}	$K(\rho_{eq})$	$E_A(\rho_{eq})$
0.0	0.198	207.84	-15.05	0.265	232.35	-18.25
0.2	0.193	195.34	-13.82	0.259	228.54	-16.74
0.4	0.165	142.33	-9.93	0.226	177.49	-12.38
0.6	0.120	85.28	-4.44	0.172	96.1	-5.89

FIGURES

FIG. 1. Diagrams of the microscopic 3BF adopted in the present calculation (see Ref. [11]). Diagram (c) was not included.

FIG. 2. Energy per nucleon of asymmetric nuclear matter in the range $0 \leq \beta^2 \leq 1$ at four densities as compared to the parabolic fits (straight lines) obtained from the first three values of β (0.0, 0.2, 0.4). Left panel : BHF predictions using AV_{18} plus the 3BF. Right panel: BHF results with only pure AV_{18} 2BF.

FIG. 3. Symmetry energy vs density. The left panel shows the comparison among different approaches: the BHF predictions with 3BF (upper solid curve) and without 3BF (lower solid curve) are obtained from the slopes of Fig. 2 (while symbols are the values approximated by Eq. (3)); the long-dash curve corresponds to the result of DBHF approach from Ref. [20]. The short dash is that of BHF calculation using the phenomenological Urbana 3BF in Ref. [19], where E_{sym} is obtained from Eq. (3). The dotted curve is the prediction of relativistic Hartree-Fock approach taken from Ref. [23]. Right panel shows simple parametrizations of the present results with (solid line) and without (dashed line) 3BF.

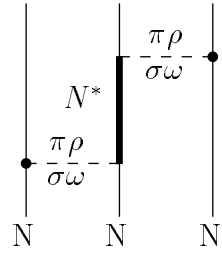
FIG. 4. Proton and neutron mean fields in asymmetric nuclear matter at $\rho = 0.17 \text{ fm}^{-3}$ for five different asymmetries. Left part shows the proton mean-field (upper panel) and the neutron one (lower panel), respectively, vs. momentum using AV_{18} plus the 3BF. Right part shows the corresponding results without the 3BF.

FIG. 5. The same as in Fig. 4 for $\rho = 0.34 \text{ fm}^{-3}$.

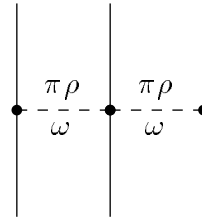
FIG. 6. Left panel: Isospin variation of proton and neutron mean fields at a fixed momentum $k = 0$ for two densities $\rho = 0.17$ and 0.34 fm^{-3} . Right panel: isospin dependence of proton and neutron effective masses calculated at their respective Fermi momenta. The results in both panels are calculated using AV_{18} plus the 3BF.

FIG. 7. Proton fraction in β -equilibrium nuclear matter calculated in the BHF approximation with 2BF (AV_{18}) and 2BF plus 3BF ($AV_{18} + 3BF$) in comparison with a variational calculation using Urbana 2BF and 3BF ($UV_{14} + UVII$). The dashed horizontal line is the threshold for direct URCA processes estimated in Ref.[34]

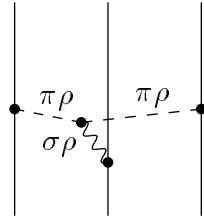
(a)



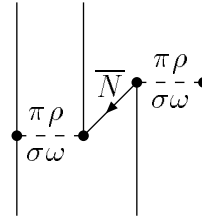
(b)

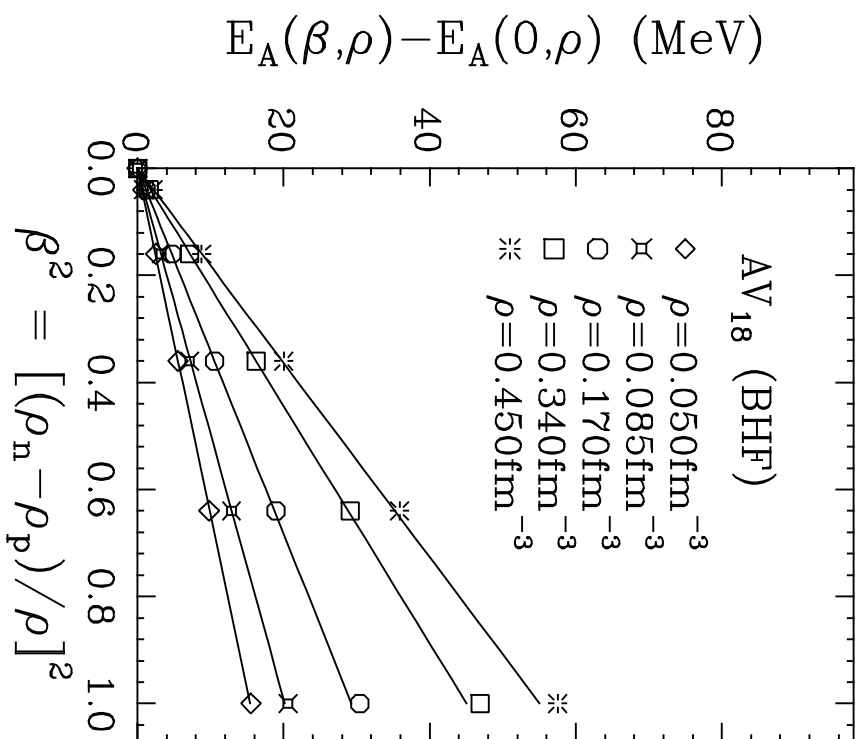
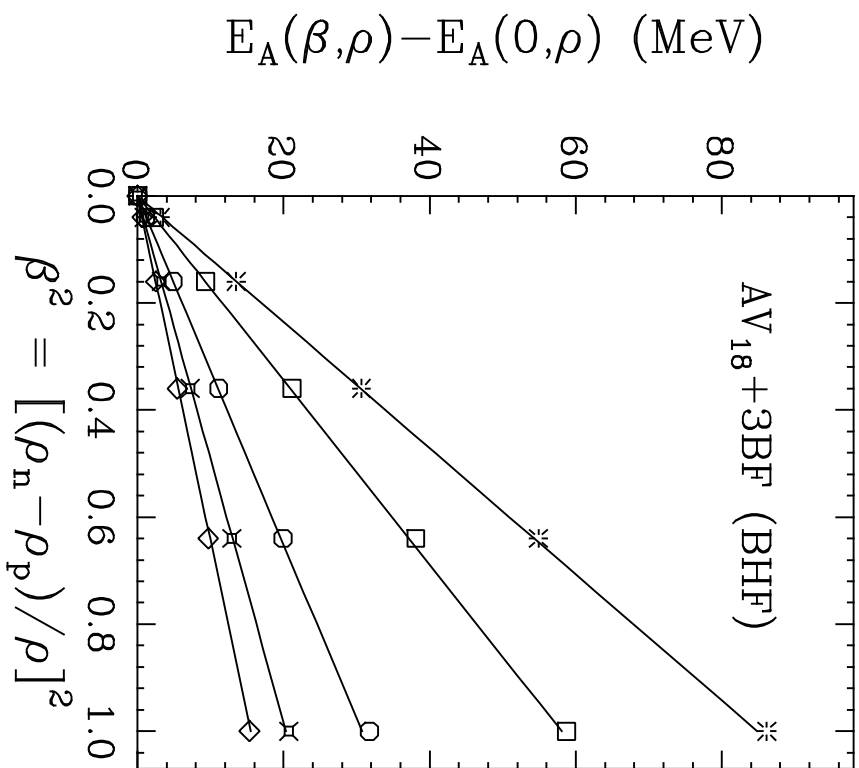


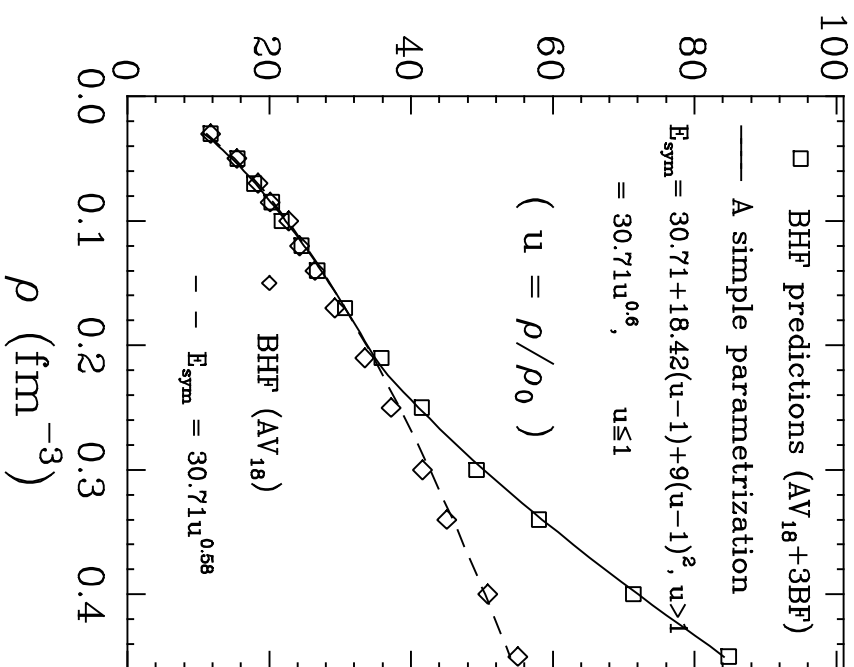
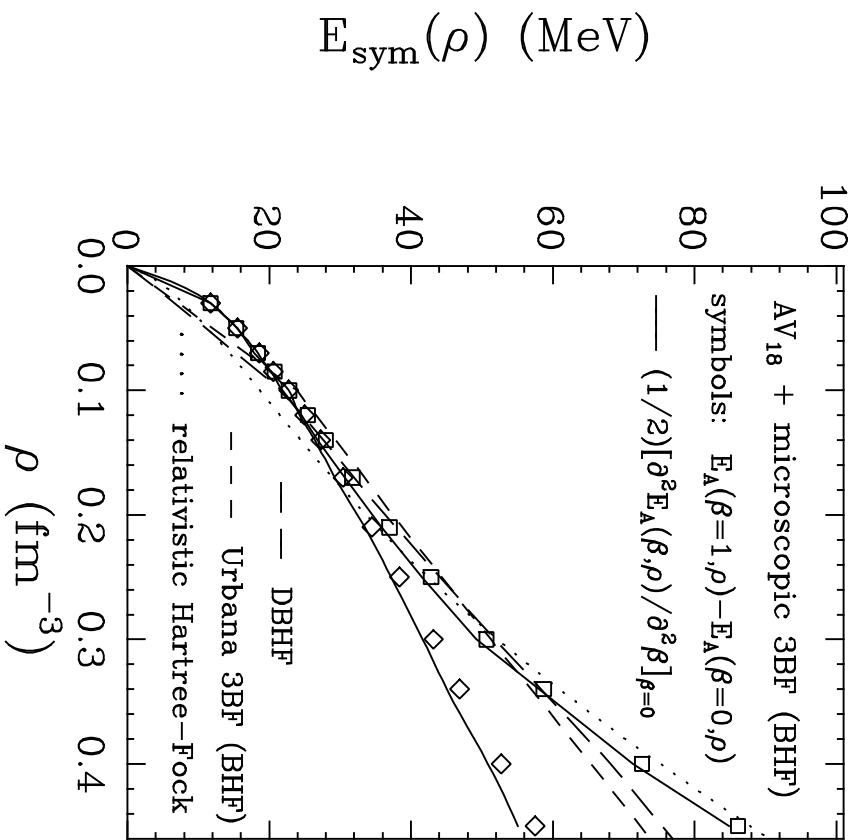
(c)



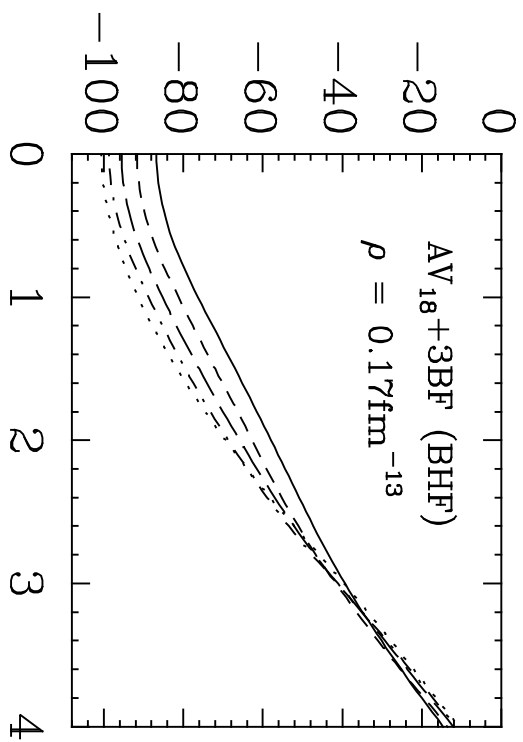
(d)





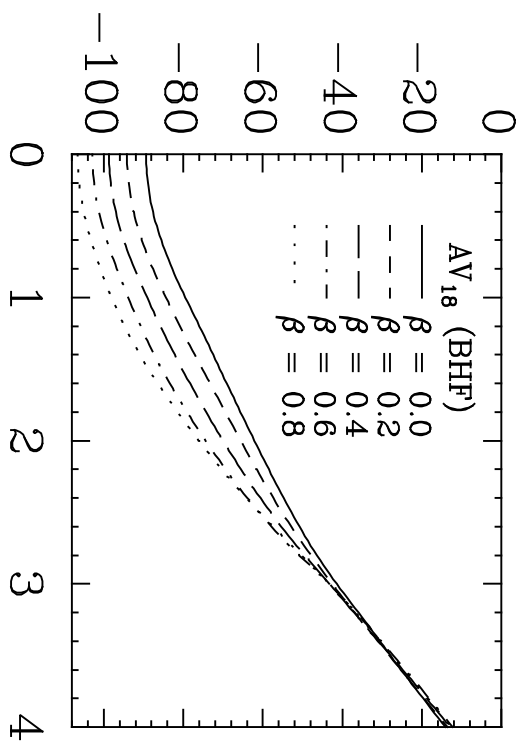


$U_p(k)$ (MeV)

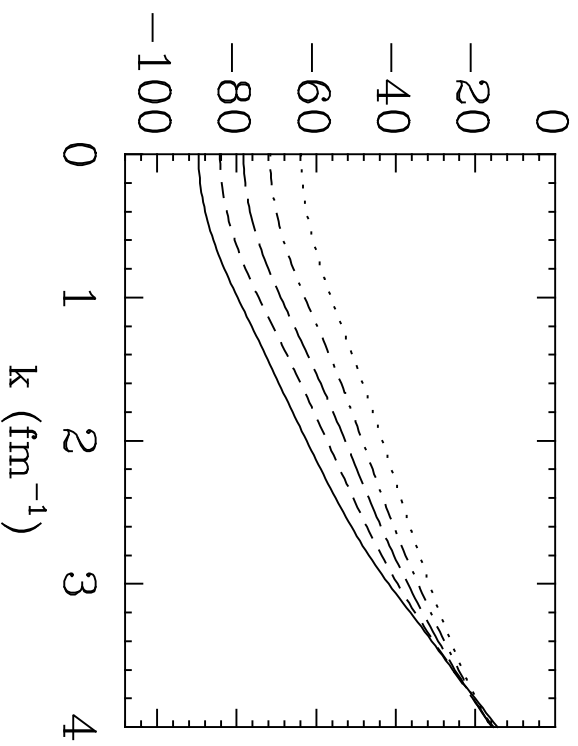
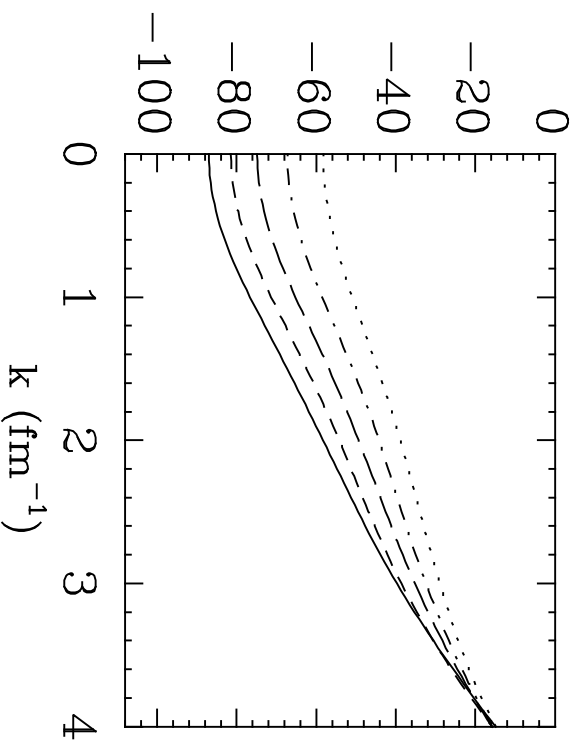


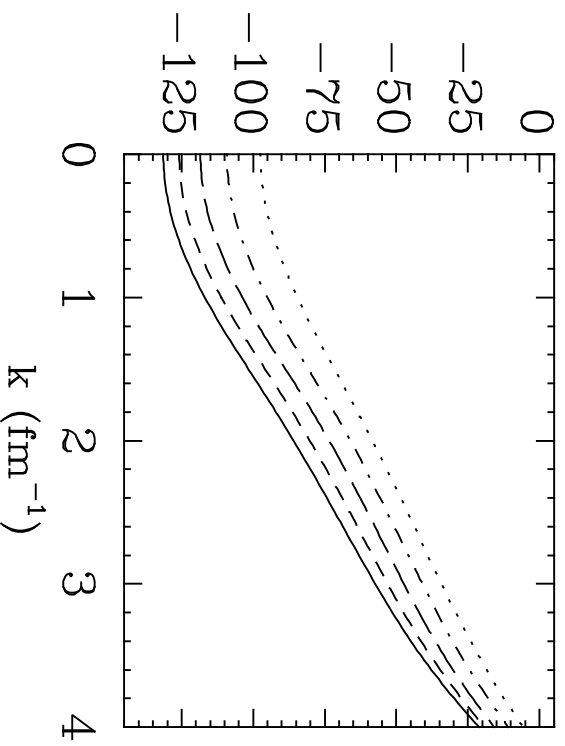
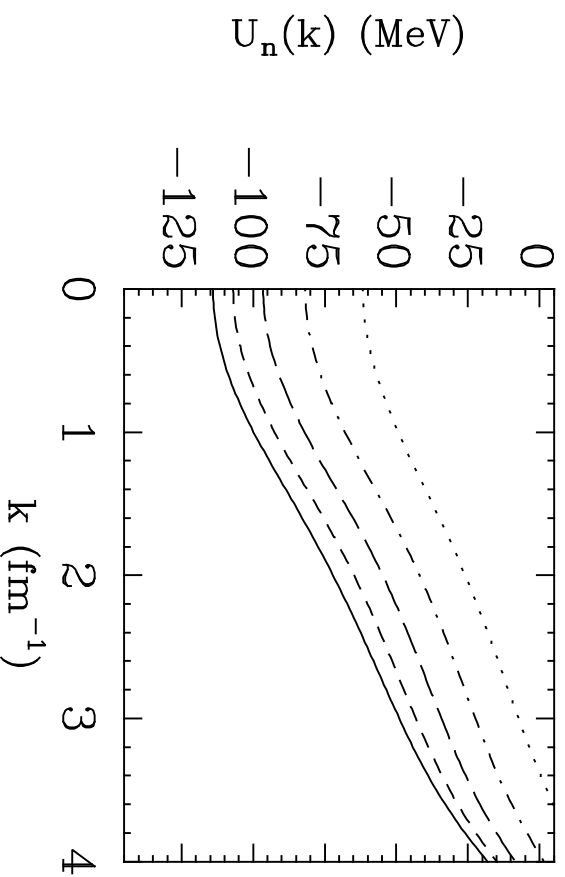
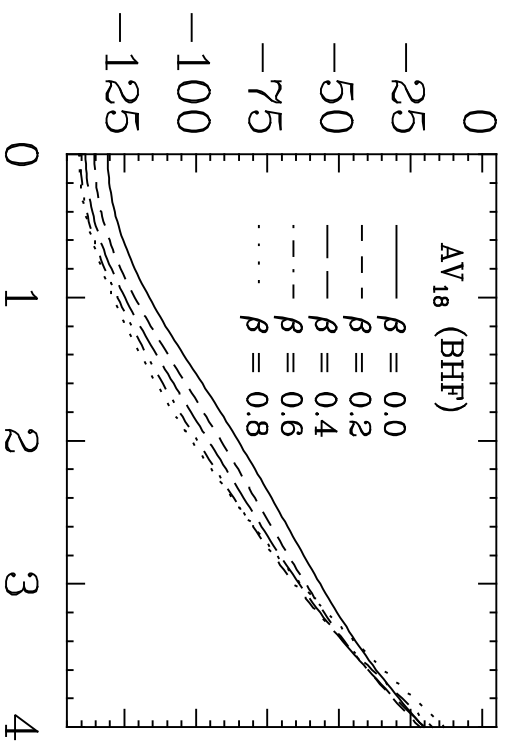
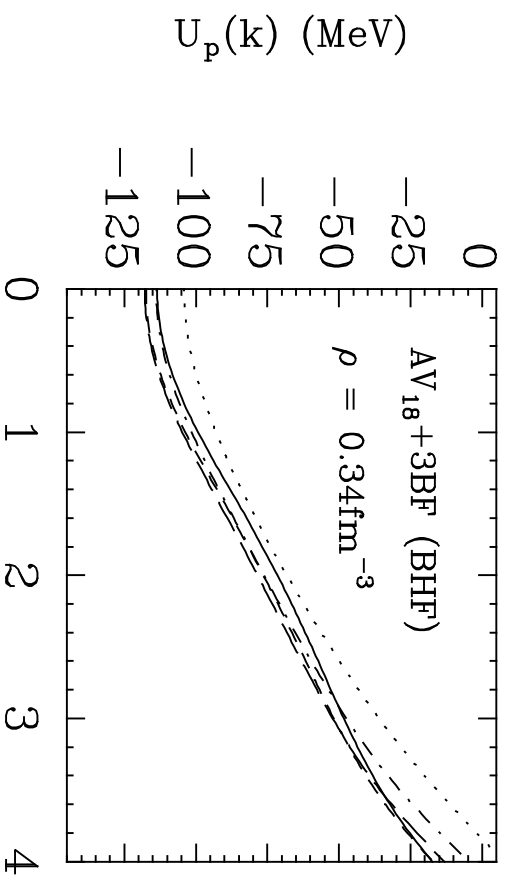
AV₁₈ (BHF)

- $\beta = 0.0$
- - $\beta = 0.2$
- · - $\beta = 0.4$
- · · $\beta = 0.6$
- · · $\beta = 0.8$

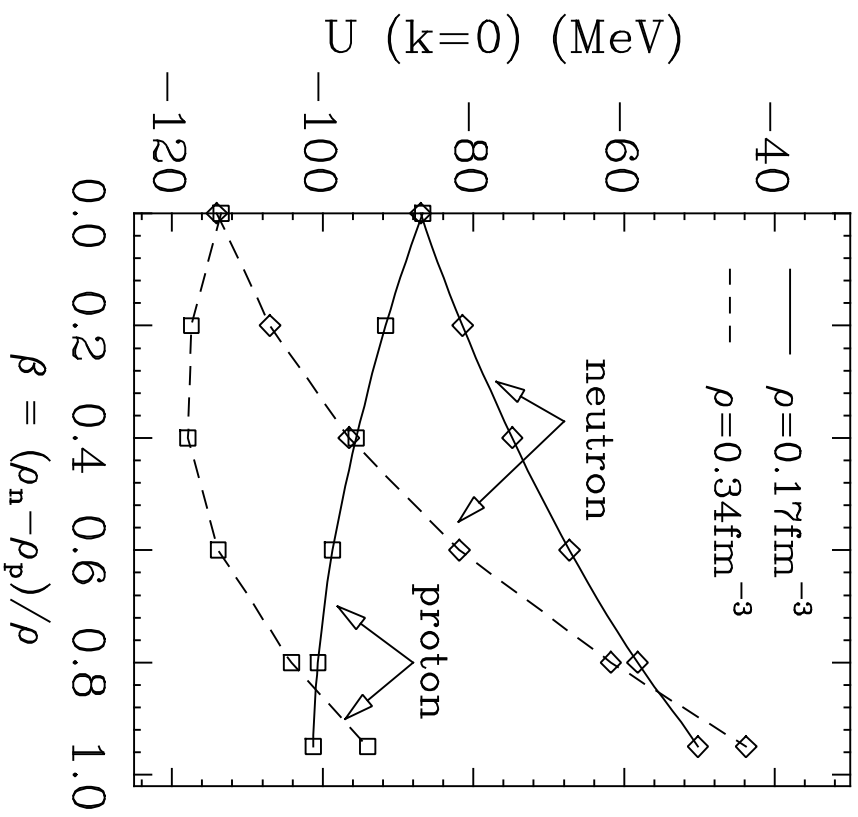


$U_n(k)$ (MeV)





$AV_{18} + 3BF$



$AV_{18} + 3BF$

